Published in final edited form as:
Nat Neurosci. 2009 March ; 12(3): 303–310. doi:10.1038/nn.2267.

Role of the synaptic ribbon in transmitting the cone light response

Skyler L Jackman[1,4], **Sue-Yeon Choi**[2,4,5], **Wallace B Thoreson**[3,4], **Katalin Rabl**[3,5], **Theodore M Bartoletti**[3], and **Richard H Kramer**[2]

[1]Department of Physics, University of California Berkeley, Berkeley, California 94720, USA

[2]Department of Molecular and Cell Biology, University of California Berkeley, Berkeley, California 94720, USA

[3]Department of Ophthalmology and Visual Sciences, University of Nebraska Medical Center, Omaha, Nebraska 68198, USA

Abstract

Cone photoreceptors distinguish small changes in light intensity while operating over a wide dynamic range. The cone synapse encodes intensity by modulating tonic neurotransmitter release, but precise encoding is limited by the quantal nature of synaptic vesicle exocytosis. Cones possess synaptic ribbons, structures that are thought to accelerate the delivery of vesicles for tonic release. Here we show that the synaptic ribbon actually constrains vesicle delivery, resulting in a maintained state of synaptic depression in darkness. Electron microscopy of cones from the lizard *Anolis segrei* revealed that depression is caused by the depletion of vesicles on the ribbon, indicating that resupply, not fusion, is the rate-limiting step that controls release. Responses from postsynaptic retinal neurons from the salamander *Ambystoma tigrinum* showed that the ribbon behaves like a capacitor, charging with vesicles in light and discharging in a phasic burst at light offset. Phasic release extends the operating range of the cone synapse to more accurately encode changes in light intensity, accentuating features that are salient to photopic vision.

From the first glimmer of dawn, through the brightest light of midday, to the fading glow of sunset, human vision depends primarily on cone photoreceptors. The cone outer segment generates a voltage signal that is finely graded over the broad range of light intensities encountered during the day, as the number of photons absorbed ranges over ~6 orders of magnitude[1]. At the other end of the cell, the cone synaptic terminal possesses voltage-gated Ca^{2+} channels that transform the voltage signal into a change in the local Ca^{2+} concentration, which alters the rate of neurotransmitter release from maximal in darkness to minimal in bright light[2,3]. Because neurotransmitter is packaged in synaptic vesicles that are exocytosed in a quantal manner, the dynamic range of vesicle release rates governs how precisely light intensity is signaled to postsynaptic neurons and ultimately limits the capabilities of cone-mediated vision[4].

Correspondence should be addressed to R.H.K. (rhkramer@berkeley.edu).
[4]These authors contributed equally to this work.
[5]Present address: Department of Ophthalmology, University of California San Francisco, San Francisco, California 94143, USA.

AUTHOR CONTRIBUTIONS

S.L.J., S.-Y.C., W.B.T. and R.H.K. conceived the experiments; S.L.J. and S.-Y.C. performed the imaging experiments and analyzed the data; K.R., T.M.B. and W.B.T. carried out the electrophysiology experiments; S.L.J. performed data analysis and modeling; and S.L.J. and R.H.K. co-wrote the paper.

Note: Supplementary information is available on the Nature Neuroscience website.

The cone terminal has been thought to serve as a relay that reliably converts light-evoked voltage signals into changes in tonic neurotransmitter release with no time-dependent changes. However, recent studies of rod, cone and bipolar cell ribbon synapses have revealed that neurotransmitter release is not strictly tonic, but rather occurs through both transient (phasic) and sustained (tonic) processes[5,6]. The two modes of release may occur at distinct ribbon and nonribbon locations[7], but it has also been suggested that the shift from phasic to tonic results from a progressive change in the availability of vesicles at a single site, the synaptic ribbon[6,8,9]. Although the mechanisms of phasic and tonic release are still uncertain, the two modes of release suggest that ribbon synapses do not faithfully relay voltage. Instead, they accentuate dynamic changes in membrane potential, thereby high-pass filtering the synaptic output.

The synaptic ribbon is the primary site of neurotransmitter release from cones. Synaptic ribbons are anchored to the membrane at active zones, where they tether hundreds of vesicles in close proximity to Ca^{2+} channels, enabling small voltage changes to efficiently control exocytosis[10]. Vesicles presumably descend along the ribbon from the cytoplasm toward the surface membrane. Whether they diffuse passively or are propelled by a molecular motor is unclear, and whether the ribbon participates in biochemical 'priming' of vesicles for membrane docking and fusion is unknown. However, because ribbons are found only in tonically releasing neurons (rods, cones, bipolar cells and hair cells), it has been proposed that the ribbon serves to accelerate the continual delivery of vesicles to meet the demands of tonic release[11,12].

We examined the transmission of the light response by the cone synapse and evaluated the role of the synaptic ribbon. By measuring the intraterminal Ca^{2+} concentration, the Ca^{2+} dependence of neurotransmitter release and the distribution of synaptic vesicles on the ribbon, we found that the ribbon was depleted of synaptic vesicles in darkness, leading to a maintained state of synaptic depression. In light, the ribbon was reloaded with vesicles, resulting in a phasic burst of release on return to darkness. The synaptic ribbon thus operates like a leaky capacitor, generating a transient signal (phasic release) that amplifies changes in illumination, superimposed on a sustained signal (tonic release) that encodes the background level of light.

RESULTS

The concentration of Ca^{2+} in the cone terminal

To understand how the cone terminal transmits the light response, we started by measuring the intraterminal Ca^{2+} concentration in light and darkness using ratiometric Ca^{2+} imaging. We monitored Ca^{2+} concentration in darkness with 2-photon laser-scanning microscopy, employing infrared light to excite dye fluorescence in cone terminals while minimizing phototransduction in outer segments[13]. Cone terminals loaded with the Ca^{2+} indicator dye fura-2 AM were imaged in retinal slices fromthe all-cone retina of the anole lizard (*Anolis segrei*)[14]. We found that the terminals of most cones had a Ca^{2+} concentration that was higher in darkness (Fig. 1a–c) than after prolonged white-light illumination (Fig. 1d–f), with the highest Ca^{2+} concentration occurring at the ribbon end of the terminal. Voltage-clamp depolarization of the cone also elicited an increase in Ca^{2+} at the ribbon end (Fig. 1g–i), which is consistent with immunolocalization of Ca^{2+} channels adjacent to synaptic ribbons[15,16]. Repeated laser scanning of cone terminals in darkness had no effect on Ca^{2+} concentration, confirming that the imaging procedure did not confound Ca^{2+} measurements by inadvertently triggering phototransduction. Examples of cone terminals (Fig. 1j) showed that some had a steep Ca^{2+} gradient in darkness. In those terminals, white light stimulation reduced the Ca^{2+} concentration near the membrane, collapsing the gradient (Fig. 1k). Other cone terminals did not have a Ca^{2+} gradient and showed little change in Ca^{2+} concentration with illumination, presumably as a consequence of cell damage during retinal slicing.

We quantified the dark level of Ca^{2+} by averaging Ca^{2+} profiles from those terminals with a substantial light response, excluding terminals that were unresponsive. We used a >5% decline in overall Ca^{2+} after light stimulation as a criterion for responsiveness. Average profiles showed a peak Ca^{2+} concentration at the ribbon end of the terminal of ~600 nM in darkness and ~250 nM in bright light (Fig. 1l). The measured peak submembrane Ca^{2+} concentration in darkness was underestimated, owing to the limited spatial resolution of light microscopy. The Ca^{2+} ionophore ionomycin elevated the Ca^{2+} concentration uniformly throughout the terminal, indicating that influx through Ca^{2+} channels is necessary for the Ca^{2+} gradient. As expected, removing extracellular Ca^{2+} reduced the intraterminal Ca^{2+} concentration to <100 nM throughout the terminal. The uniform Ca^{2+} distribution with ionomycin and Ca^{2+}-free saline suggests that the Ca^{2+} gradient in darkness results from Ca^{2+} influx through localized channels and not from Ca^{2+} removal through localized extrusion mechanisms such as the plasma membrane Ca^{2+} ATPase[17].

Ca^{2+} dependence of neurotransmitter release

To investigate the Ca^{2+}-dependence of neurotransmitter release, we employed paired electrophysiological recordings from cones and retinal bipolar cells, enabling measurement of the excitatory postsynaptic currents (EPSCs) elicited by a rise in presynaptic Ca^{2+}. For these experiments, we used cones from the tiger salamander (*Ambystoma tigrinum*) retina because their compact structure[17] allows for a more effective voltage-clamp of the synaptic terminal than lizard cones, which have a long axon separating the inner segment from the terminal[18]. Depolarizing a salamander cone from −70 to −10 mV evoked an inward Ca^{2+} current, which in turn elicited an EPSC in a hyperpolarizing bipolar cell (HBC). Despite the sustained presynaptic Ca^{2+} current, the evoked EPSC was transient, decaying from a large phasic response to a small tonic response (Fig. 2a). Presynaptic capacitance measurements demonstrate that EPSCs accurately reflect cone exocytosis[5]. Therefore, a sustained Ca^{2+} increase in cones triggers both phasic and tonic release processes.

To quantify the Ca^{2+}-dependence of each of these processes, we recorded EPSCs while controlling intraterminal Ca^{2+} with 'caged Ca^{2+}'. The photolyzable Ca^{2+}-chelator DM-nitrophen[19] was delivered via whole-cell patch pipette along with the Ca^{2+} indicator dye Oregon Green BAPTA-6F (OGB-6F). A flash of ultraviolet light increased the presynaptic Ca^{2+} concentration, evoking an EPSC in an HBC that we recorded (Fig. 2b).We calculated quantal release from the cone synapse (Fig. 2c) by deconvolving the EPSC with the waveform of the averaged mEPSC[20] (Fig. 2b). The response triggered by a sustained rise in Ca^{2+} could be attributed to two components of release, a phasic component that decayed over a double exponential time course and a tonic component that persisted for hundreds of milliseconds after the uncaging flash. Integrating the release rate over time showed that the abrupt rise in Ca^{2+} triggered the prompt fusion of a pool of ~120 vesicles (phasic release) while simultaneously enhancing tonic release (Fig. 2d).

We varied the intensity of the uncaging light to evoke a range of abrupt jumps in presynaptic Ca^{2+} concentration (Fig. 3a,b).We found that the phasic and tonic release processes were regulated similarly by Ca^{2+}. Both had Ca^{2+} thresholds of <1 μM and the rates of both processes increased linearly over the narrow range of Ca^{2+} concentrations that we tested. However, the tonic release rate was ~tenfold slower than the phasic release rate (Fig. 3a).

To provide an independent measure of the Ca^{2+} dependence of tonic release, we added ionomycin to anole cones and varied the extracellular Ca^{2+} to 'clamp' Ca^{2+} at different intracellular concentrations[13]. The Ca^{2+} concentration was measured with fura-2 and the tonic release rate was determined by measuring the loss of the synaptic vesicle dye FM1-43 (Supplementary Fig. 1 online). The relationship between ionomycin-elevated Ca^{2+} and release in anole cones (Fig. 3b) was consistent with the relationship between photolytically elevated

Ca^{2+} and tonic release in salamander cones, suggesting that both measurements reflect the same tonic release process, even though they were obtained with different methods in different species.

It is possible that tonic and phasic release are mediated by distinct biochemical mechanisms that both have a linear dependence on Ca^{2+} and a low threshold. However, a simpler explanation is that the two processes utilize the same Ca^{2+} sensor for exocytosis and differ only in the number of vesicles that are available for release. In this scenario, a readily releasable pool is depleted quickly by the initial burst of phasic release, leaving a smaller pool to mediate tonic release, but which nonetheless occurs by the same mechanism. This model contrasts with the calyx of Held, where synchronous and asynchronous release have different Ca^{2+} dependencies because they use different Ca^{2+} sensors[21].

Which process, phasic or tonic, accounts for transmitter release from cones in darkness? Assuming a submembrane Ca^{2+} concentration of 600 nM (Fig. 1), the phasic process predicts a dark release rate of ~2,400 vesicles per s and the tonic process predicts ~230 vesicles per s (Fig. 3a,b). Given that a salamander HBC contacts 2–5 ribbons from each presynaptic cone[22], our uncaging experiments predict a dark release rate of 470–1,200 vesicles per ribbon per s for the phasic process and 45–110 vesicles per ribbon per s for the tonic process. The measured release rate from salamander cones is ~500 vesicles per s in darkness[13] and cone terminals possess ~13 ribbons[23]. Thus, each ribbon releases ~40 vesicles per s in darkness, which is consistent with the tonic rather than the phasic process.

Distribution of synaptic vesicles on the ribbon

The transition from phasic to tonic release during a depolarizing step could stem from depletion of synaptic vesicles available for release. Because the tonic mechanism appears to govern release in darkness, we expect that keeping the retina in darkness would result in the depletion of synaptic vesicles near release sites. To test this hypothesis, we directly visualized cone synapses with electron microscopy.

Retinal slices from anoles were dark adapted, light adapted or exposed to Ca^{2+}-free saline for 30 min before electron microscopy preparation. Cone terminals possessed synaptic ribbons with closely associated vesicles in all three treatments (Fig. 4a and Supplementary Fig. 2 online). However, a difference emerged when we mapped and superimposed the vesicle positions from many ribbons (Fig. 4b). Ribbons in dark-adapted cones had a clear deficit of vesicles, particularly within 200 nm of the base of the ribbon, near release sites (Fig. 4c). Comparison of 115 ribbons from each treatment showed little difference in either the total number of vesicles per ribbon (Fig. 4d) or the average ribbon length (Supplementary Fig. 3 online), but a highly significant difference ($P < 0.0001$) at the base of the ribbon, where dark-adapted cones had 3.7-fold fewer vesicles than light-adapted cones (Fig. 4e). This is less than the tenfold difference expected from our comparison of tonic and phasic release rates (Fig. 3), but this discrepancy could arise from systematic over-counting of vesicles on depleted ribbons (see Supplementary Fig. 4 online for a discussion of electron microscopy error). Treatment with Ca^{2+}-free saline significantly increased vesicle number not only at the ribbon base ($P < 0.0001$), but also on the entire ribbon ($P < 0.01$). These results indicate that synaptic vesicles are depleted at the base of the ribbon, implying that vesicle release outpaces replenishment. Therefore, the resupply of vesicles to the base of the ribbon, rather than fusion with the plasma membrane, is the rate-limiting step in tonic neurotransmitter release in darkness.

Effect of vesicle depletion on synaptic signaling

To evaluate the effect of vesicle depletion on synaptic transmission of the cone light response, we considered a scenario in which vesicles bind to the ribbon, descend into a release zone at

the base of the ribbon and then fuse with the plasma membrane in a Ca^{2+}-dependent manner (**Supplementary Movie 1** online). In darkness, when the Ca^{2+} concentration is high near the membrane, fusion outpaces vesicle descent and the release zone becomes depleted. In light, the Ca^{2+} concentration falls, slowing fusion without affecting descent. This allows the base of the ribbon to repopulate with vesicles. At light offset, the fully populated ribbon is suddenly exposed to elevated Ca^{2+}. At first exocytosis resumes at a high rate, but then the base of the ribbon becomes depleted and release subsides to the tonic dark rate.

All neurons receiving input from cones show a transient 'off ' response after a light flash[24]. Depolarizing bipolar cells (DBCs) had a hyperpolarizing transient and HBCs had a depolarizing transient (Fig. 5a), as did horizontal cells (Supplementary Fig. 5 online). In a subset of HBCs, glutamate receptors recover from desensitization during the light response and this accounts for the depolarizing overshoot that occurs on return to darkness when cone glutamate release resumes[8]. In other HBCs[8], horizontal cells[25] and DBCs[26], however, the kinetics of recovery from receptor desensitization cannot account for the off response, suggesting a presynaptic mechanism.

We propose that the accumulation of vesicles on the ribbon during a light flash generates these off responses. In darkness, the group of cones contacting an HBC collectively released 300 vesicles per s, as determined by deconvolution of the HBCs synaptic current (Fig. 5b). Because the dark release rate is limited by vesicle resupply and not by fusion, the resupply rate must also be 300 vesicles per s. During illumination, release slowed to 100 vesicles per s (Fig. 5b). Therefore, the ribbons should have amassed 400 extra vesicles during the 2-s light flash. Matching this prediction, we found that 390 vesicles were released in 200 ms of light offset (Fig. 5b).

To further test whether accumulation of vesicles on the ribbon underlies the off transient response, we measured how light-flash duration affects the magnitude of the response. The depleted ribbon model predicts that more vesicles will accumulate on the ribbon with longer flashes of light, until the ribbon is saturated with vesicles. We found that the off transient response increased with flash duration and then saturated (Fig. 6a). On average, the off response increased with a time constant of 1.7 s (Fig. 6b), although even a 100-ms flash generated a prominent off response. The off response reached a plateau at ~5 s, consistent with saturation of vesicles on ribbons (Fig. 6b).

To confirm that the off response is mediated by a change in presynaptic release, we measured capacitance changes in the cone terminal resulting from the increase in membrane surface area that occurs during exocytosis. The cone was initially held at the dark membrane potential of −35 mV, stepped to −70 mV to simulate light-induced hyperpolarization and then stepped to −10 mV to trigger exocytosis of the releasable pool of vesicles (Fig. 6c). Increasing the duration of the hyperpolarizing step increased the magnitude of the capacitance response, but responses began to saturate after several seconds. We calculated the number of vesicles released using a capacitance value of 57 aF per vesicle[27]. The presynaptic capacitance signal (Fig. 6d) and the postsynaptic off response (Fig. 6b) grew at similar rates with increasing flash duration, and both signals could be fit to our model of vesicle depletion and resupply (see Supplementary Fig. 6 and Supplementary Methods online). However, a fast component of recovery was evident in the capacitance measurement, but not in the postsynaptic response. This could reflect a small contribution from presynaptic release at nonribbon sites[7] or recovery from postsynaptic desensitization[8]. The kinetics of vesicle accumulation resembles recovery from paired-pulse depression by the cone synapse[25], an indicator of changes in the size of the readily releasable pool. The total number of vesicles that accumulate on a ribbon during a prolonged hyperpolarizing step (56 vesicles) was consistent with the capacity of the base of a fully populated ribbon (65 vesicles), as determined by our electron microscopy data and

morphological analysis of the salamander cone synapse[23] (for calculations see Supplementary Table 1 and Supplementary Table 2 online).

Other possible mechanisms for the off response have been proposed. For example, inhibition of cone Ca^{2+} channels by exocytosed protons[28] or feedback from horizontal cells[29] could decrease during the light response, enhancing release on return to darkness. However, prominent off responses were seen with HEPES-buffered saline (Fig. 5b), which blocks both of these effects[28,29]. Some cones show a depolarizing afterpotential at light offset[24], but this response was too small and too slow to account for the postsynaptic off response (Supplementary Fig. 5).

Phasic release improves the encoding of light intensity

Cones generate a graded response to increments of light and this causes a graded decrease in synaptic vesicle release. Brighter light more effectively slows release, resulting in the accumulation of more synaptic vesicles on the synaptic ribbon. This suggests that a brighter light flash will produce a larger off response in postsynaptic cells. To test this prediction, we recorded responses to various flash intensities in HBCs. We found that the peak off response following a 2-s flash increased over ~4 log units of intensity before saturating with very bright light (Fig. 7a). Furthermore, the magnitude of the off response after the light flash increased over the same intensity range as the response during the light flash (that is, the 'on' response). This is consistent with graded suppression of tonic release underlying the on response and phasic release of accumulated vesicles underlying the off response. Throughout this intensity range, however, the magnitude of the off response was always 3–4-fold larger than the on response. Phasic release at light offset employs a larger range of synaptic vesicle releases rates and could allow more accurate encoding of light intensity.

We compared the encoding capabilities of tonic and phasic release rates. Assuming that vesicle release is stochastic and therefore obeys Poisson statistics, a salamander cone tonically releasing 500 vesicles per s in darkness[13] can transmit only ~13 distinguishable levels of steady light before release is suppressed completely (Fig. 7b; for calculations, see **SupplementaryMethods**). By increasing the release rate to ~3,350 vesicles per s (the phasic release rate after a 2-s light flash, average response from 6 HBCs), phasic release improved the encoding of fine gradations of light, allowing for ~33 distinguishable decrements in light (Fig. 7c).

DISCUSSION

Function of the synaptic ribbon in cones

At each cone active zone, hundreds of voltage-gated Ca^{2+} channels, an unknown number of vesicle fusion sites and a single synaptic ribbon assemble in a stereotypic manner to control neurotransmitter release[10,30,31]. In darkness, the depolarized membrane potential opens Ca^{2+} channels, elevating the Ca^{2+} concentration at the active zone and supporting exocytosis of synaptic vesicles at fusion sites. Diffusion of Ca^{2+} away from the mouth of the channels and buffering by Ca^{2+}- binding proteins establish a Ca^{2+} gradient in the cytoplasm that diminishes with distance from the membrane. Thus, any Ca^{2+}-regulated process that occurs should be affected differentially along the ribbon surface as it extends from the membrane.

Studies on the bipolar cell ribbon synapse showed that elevated Ca^{2+} concentrations accelerate vesicle resupply[32]. This implies that Ca^{2+} regulates the interaction of vesicles with the ribbon as well as regulating fusion with the plasma membrane. Our experiments in cones suggested that resupply is unaffected by physiological levels of Ca^{2+} because the rate of vesicle accumulation in the light, when cytoplasmic Ca^{2+} is low, was nearly identical to the tonic

release rate in darkness, when cytoplasmic Ca^{2+} is high. It is possible that this reflects a fundamental difference in the resupply process in cones and bipolar cells. Alternatively, the modest Ca^{2+} elevation in cones in darkness may be too localized to the surface membrane to influence Ca^{2+} sensors that might be located further up the ribbon.

The synaptic ribbon has been portrayed as a 'conveyor belt' for transporting vesicles from the cytoplasm to release sites[33,34]. Vesicles appear to exit the synaptic ribbon exclusively at the membrane end[35]. Depletion on the ribbon in darkness indicates that vesicles near the base have either descended more rapidly than those at the top, fused directly to the plasma membrane along the flanks of the synaptic ridge or have detached before reaching the plasma membrane. The ribbon has also been thought to accelerate the delivery of vesicles to release sites[11,12]. However, our calculations suggest that, in comparison with vesicle delivery by free diffusion through the cytoplasm, the ribbon actually slows delivery, thereby restraining release. In darkness, vesicles are released from anole cones at 250 vesicles per s, or 10 vesicle per ribbon per s (ref. [36]). Given the concentration of vesicles in cone terminals (~2,000 vesicles per μm^2) and their cytoplasmic diffusion coefficient (0.11 $\mu m^2\ s^{-1}$)[14], freely diffusing vesicles should collide with an area the size of a ribbon-associated active zone (200 nm wide by 500 nm long) at 75 vesicles per s, faster than the observed release rate at individual ribbons. Unlike cytoplasmic vesicles, which move in three dimensions, ribbon-bound vesicles are constrained to move in two dimensions, predicting an even faster active zone encounter rate of 180 vesicles per s. Therefore, although the ribbon may prime vesicles to make them fusion competent[36], the calculations suggest that it slows rather than speeds the delivery of vesicles to release sites and limits the fusion rate. We speculate that slowing delivery enables the ribbon to serve as a 'timing belt', making the interval between sequential fusion events more regular than if vesicles were resupplied directly from the cytoplasm. Theoretical considerations suggest that small sensory stimuli would be undetectable to the visual system unless the photoreceptor terminal possessed a mechanism for regularizing release[37].

Recent studies have shown that the synaptic ribbon in bipolar cells serves as a platform for promoting compound fusion during strong depolarizations[38]. Multivesicular release, possibly mediated by compound fusion, has been observed in a variety of ribbon synapses[39,40]. None of our electron microscopy images from cones in darkness or in steady light showed structures that were indicative of compound fusion. However, it is possible that compound fusion might be more prevalent during the phasic burst of release that occurs on transition from light to darkness. It has also been shown that release at ribbon synapses can occur at extra-ribbon locations[7]. The quantitative agreement between the vesicle storage capacity of the ribbon and the magnitude of postsynaptic responses suggests that the ribbon mediates release in response to our light and dark stimuli, but it is possible that larger depolarizations might recruit extra-ribbon release.

Synaptic encoding of steady and changing light

At most conventional synapses, vesicle release is triggered by the intermittent rise in Ca^{2+} that occurs during action potentials. The cone synapse also uses Ca^{2+} as a trigger for release, but adds a second layer of control by dynamically varying the number of vesicles on the ribbon that are available for release. The release rate is minimal when a depleted ribbon is exposed to low Ca^{2+}; that is, during a step from darkness to bright light. The release rate is maximal when a fully populated ribbon is exposed to high Ca^{2+}, during a step from bright light to darkness. Between these two extremes, the synapse can finely tune its release rate by varying the Ca^{2+} signal and the available vesicle pool, optimizing the encoding of fine differences in light intensity. Studies of other ribbon synapses show that strong depolarization decreases the size of the readily releasable pool of vesicles, leading to synaptic depression[41–43]. Our results

explain the physiological importance of this phenomenon in cones and demonstrate directly that it is mediated by depletion of synaptic vesicles on the ribbon.

Our results indicate that the rate-limiting step that controls cone neurotransmitter release switches from vesicle resupply during tonic transmission to Ca^{2+}-dependent fusion during phasic transmission. We propose that this switch also improves the synaptic encoding of light intensity. Control of the release rate by vesicle resupply distances tonic transmission from noisy signals generated by the stochastic opening of Ca^{2+} channels. Also, controlling tonic release via resupply rather than by fusion probably reduces the intrinsic noise of release. Vesicle fusion is a stochastic, all-or-none event, whereas descent along the ribbon and docking to the membrane involves multiple steps, which should make the overall rate more consistent by averaging the fluctuations of individual steps[44]. In contrast, controlling phasic release at the fusion step ensures that the synaptic signal representing changing light is transmitted as rapidly as possible.

The consequence of phasic release is a large and rapid off response in all neurons that are postsynaptic to cones. Most bipolar cells receive either direct or indirect input from both rods and cones[22]. Synaptic input driven by the rod light response, which decays very slowly after light offset, can obscure the cone-mediated off response[45]. However, during daylight hours, the retina is exposed to background illumination that often saturates rod phototransduction. Under these photopic conditions, the cone-mediated off response becomes a prominent feature of the bipolar cell light response, contributing strongly to transient responses in downstream neurons in the visual system.

The response in postsynaptic cells increases as a function of both flash intensity and duration. Therefore, rather than encoding absolute intensity, the off response is a history-dependent representation of the change in intensity with respect to background. The sequence of opposite polarity on and off responses increases the contrast gain of the synapse. Notably, the phasic behavior of the cone ribbon synapse augments the signaling of light decrements, but the synapse displays no equivalent transient behavior at light onset. Other processes, such as cone light adaptation[46], horizontal cell–mediated synaptic feedback[47] and glutamate receptor desensitization[8], can generate transient responses to light increments in bipolar cells. However, our results are consistent with those of previous studies[45] showing that the change in voltage in postsynaptic neurons under photopic conditions is larger at light offset than light onset. This asymmetry enables the cone synapse to encode light decrements more accurately than light increments. This is consistent with the observation that natural images show a statistical overabundance of decrements with respect to the mean brightness of a scene[48]. Thus, the phasic properties of the cone synapse may help with the detection of dark objects silhouetted against a bright background. Indeed, psychophysical studies show that human observers are more sensitive to decrements than to increments of light. The locus of this asymmetry has been tracked to early retinal processing[49] and may result from the properties of cone vesicle release elucidated in this study.

METHODS

Ca^{2+} imaging

All experiments were performed at 21–24 °C. For fura-2 loading, retinas from lizards (*Anolis segrei*) were isolated as described previously[13] using procedures approved by the University of California Berkeley Animal Care and Use Committee. Retinas were flat mounted onto nitrocellulose filter paper, sliced to a thickness of ~300 μm and loaded for 30 min in saline solution[13] containing 100 μM Fura-2 AM. Images were acquired using a two-photon confocal microscope (Zeiss) with a Ti-sapphire laser (Coherent). Intraterminal Ca^{2+} was calculated from the ratio of fura-2 fluorescence at excitation wavelengths of 700 nm and 760 nm[13]. The K_{eff}

of fura-2 binding to Ca^{2+} (180 nM) was determined *in situ* by dialyzing cones with EGTA-buffered solutions containing 132 mM KCl, 2 mM NaCl, 10 mM EGTA, 3.5 mM $CaCl_2$, 2 mM $MgCl_2$ and 20 mM HEPES (pH 7.1). Minimum and maximum ratios were obtained using similar pipette solutions with 0 mM $CaCl_2$ or 0 mM EGTA, respectively. To analyze Ca^{2+} profiles, we drew 0.5-μm-wide × 3.0-μm-long rectangles along the ribbon-to-axon axis of the terminal, abutting the ribbon end of the terminal. Data points in the traces of different experimental conditions represent the average values ± s.e.m.

For Ca^{2+} imaging with OGB, lizard retinal slices were prepared using techniques that were described previously for salamander retinas[5]. Whole-cell voltage-clamp recordings were obtained with an Optopatch amplifier using 8–15 MΩ borosilicate glass patch electrodes. The pipette solution contained 132 mM cesium gluconate, 10 mM tetraethyl ammonium chloride (TEACl), 2 mM $MgCl_2$, 1 mM $CaCl_2$, 10 mM magnesium ATP, 2 mM glucose, 0.5 mM GTP, 5 mM EGTA, 20 mM HEPES (pH 7.2) and 200 μM OGB-5N. Cones were imaged through an upright, fixed-stage microscope (Nikon E600 FN) mounted with a laser confocal scanhead (Perkin Elmer Ultraview LCI) and equipped with a CCD camera (Orca ER).

Electron microscopy

Lizard retinas were isolated in darkness and maintained for 30 min in darkness, bright white light or saline containing 0 mM Ca^{2+} and 5 mM EGTA. Retinas were fixed with 2% paraformaldehyde (wt/vol) and 2% glutaraldehyde (wt/vol) in 0.1 M phosphate buffer (pH 7.4) overnight at 4 °C. Fixed tissue was postfixed with 1% osmium tetraoxide and 1.5% potassium ferrocyanide (wt/vol) and dehydrated with a graded series of ethanol solutions. Prepared retinas were embedded in Epon 812 for transmission electron microscopy and sectioned into 70 nm thickness using a Reichert-Jung Ultracut E with a diamond knife. Sections were examined with the FEI Tecnai 12 electron microscope. Vesicle occupancy was calculated by counting vesicles lying within 120 nm of ribbons on sample sections and multiplying with a scaling factor (9.0) reflecting the length of the ribbon perpendicular to the membrane[50] and the packing density of vesicles on the fully occupied ribbon[27].

Electrophysiology

Retinal slices from the larval tiger salamander (*Ambystoma tigrinum*) were prepared as previously described[5] using procedures approved by the University of Nebraska Medical Center Institutional Animal Care and Use Committee. Whole-cell voltage-clamp recordings were obtained from cones using 10–15 MΩ patch pipettes pulled from borosilicate glass. The pipette solution contained 42 mM $CsCl_2$, 48 mM cesium gluconate, 1.9 mM $MgCl_2$, 32.9 mM HEPES, 9.4 mM TEACl, 9.4 mM magnesium ATP, 0.5 mM GTP and 5 mM EGTA (pH 7.2). Cones were voltage clamped at −70 mV using an Optopatch (Cairn Instruments) patch-clamp amplifier. For caged Ca^{2+} experiments, the pipette solution consisted of 10 mM DM-nitrophen, 5 mM $CaCl_2$, 4 mM 1,3-diaminopropane-2-ol-*N*,*N*′-tetraacetic acid, 4 mM $MgCl_2$, 26 mM cesium gluconate, 78 mM HEPES, 6.5 mM TEACl, 11 mM sodium ATP, 0.5 mM GTP, 0.5 mM OGB-6F (K_d = 3 μM) (pH 7.2). Calcium levels in flash photolysis experiments were determined by

$$\left[Ca^{2+}\right] = \left[Ca^{2+}\right]_{Rest} + K_d \times \frac{\Delta F/F}{(\Delta F/F)_{max}} \times \frac{1}{1 - \frac{\Delta F/F}{(\Delta F/F)_{max}}}$$

$[Ca^{2+}]_{Rest}$ was determined from aliquots of each solution using fura-2. $(\Delta F/F)_{max}$ was determined from the maximum fluorescence increase evoked by strong depolarizing steps. Cones were stimulated with flashes of 680-nm light (1.1×10^6 photons s^{-1} μm^{-2}), whereas

rod input onto bipolar cells was suppressed with a 480-nm background light of (1.0×10^3 photons s^{-1} μm^{-2}).

Calculating neurotransmitter release rates

Transmitter release from salamander cones was calculated by deconvolving the HBC EPSC with the waveform of the averaged miniature EPSC (mEPSC)[20]. For each cone-HBC pair, the mEPSC waveform was fit with an instantaneous rise time and exponential decay. Release from lizard cones was calculated from the rate of FM1-43 (Invitrogen) unloading from cone synapses in retinal slices[50]. Retinal slices loaded with FM1-43 were prepared as described previously[13] and transferred to Ca^{2+}-free saline containing 5 μM fura-2 AM (Invitrogen) for 30 min. Slices were imaged with an upright Nikon microscope and fluorescence was detected with an Imago Sensicam (TILL Photonics). A Lambda 10–2 filter wheel (Sutter Instruments) controlled the excitation wavelength. FM1-43 was excited with 490-nm light. Fura-2 was excited with 350- and 380-nm light. A 510 ± 10–nm emission filter was used for both dyes. *In vitro* fura-2 calibration was performed with a fura-2 Ca^{2+}-imaging calibration kit.

Modeling vesicle resupply

Vesicle resupply was modeled using Mathematica (Wolfram Research). The size of the readily releasable pool (*RRP*) was estimated from electron microscopy data as the number of ribbon-associated vesicles located in the depletion zone. To convert this number to an estimate of the maximal *RRP* (RRP_{MAX}) for a single ribbon, we multiplied by a factor of 17.65 vesicles per μm to reflect the density of vesicles along the length of a cone ribbon[27]. We assumed the driving force for resupply was a function of *RRP* and that the maximal resupply rate was equal to the rate of exocytosis in the dark (R_{Dark} = 40 vesicles per ribbon in salamander cones). To calculate vesicle resupply, we used

$$\text{Resupply} = R_{\text{Dark}}\left(1 - \frac{\text{RRP}}{\text{RRP}_{\text{MAX}}}\right)$$

Supplementary Material

Refer to Web version on PubMed Central for supplementary material.

ACKNOWLEDGMENTS

We thank D. Fortin, R. Heidelberger and F. Werblin for comments on the manuscript, R.S. Zucker for advice on Ca^{2+} imaging and R. Zalpuri for help with electron microscopy. This work was supported by grants from Research to Prevent Blindness to W.B.T. and the US National Institutes of Health to R.H.K. (EY015514) and W.B.T. (EY10542).

References

1. Dowling JE, Ripps H. Effect of magnesium on horizontal cell activity in the skate retina. Nature 1973;242:101–103. [PubMed: 4348460]
2. Baylor DA, Fuortes MGF, O'Bryan PM. Receptive fields of cones in the retina of the turtle. J. Physiol. (Lond.) 1971;214:265–294. [PubMed: 5579638]
3. Ashmore JF, Copenhagen DR. An analysis of transmission from cones to hyperpolarizing bipolar cells in the retina of the turtle. J. Physiol. (Lond.) 1983;340:569–597. [PubMed: 6310101]
4. Sterling P, Freed M. How robust is a neural circuit? Vis. Neurosci 2007;24:563–571. [PubMed: 17711602]
5. Rabl K, Cadetti L, Thoreson WB. Kinetics of exocytosis is faster in cones than in rods. J. Neurosci 2005;25:4633–4640. [PubMed: 15872111]

6. Mennerick S, Matthews G. Ultrafast exocytosis elicited by calcium current in synaptic terminals of retinal bipolar neurons. Neuron 1996;17:1241–1249. [PubMed: 8982170]
7. Midorikawa M, Tsukamoto Y, Berglund K, Ishii M, Tachibana M. Different roles of ribbon-associated and ribbon-free active zones in retinal bipolar cells. Nat. Neurosci 2007;10:1268–1276. [PubMed: 17828257]
8. DeVries SH. Bipolar cells use kainate and AMPA receptors to filter visual information into separate channels. Neuron 2000;28:847–856. [PubMed: 11163271]
9. Singer JH, Diamond JS. Vesicle depletion and synaptic depression at a mammalian ribbon synapse. J. Neurophysiol 2006;95:3191–3198. [PubMed: 16452253]
10. Heidelberger R, Thoreson WB, Witkovsky P. Synaptic transmission at retinal ribbon synapses. Prog. Retin. Eye Res 2005;24:682–720. [PubMed: 16027025]
11. Parsons TD, Lenzi D, Almers W, Roberts WM. Calcium-triggered exocytosis and endocytosis in an isolated presynaptic cell: capacitance measurements in saccular hair cells. Neuron 1994;13:875–883. [PubMed: 7946334]
12. von Kriegstein K, Schmitz F, Link E, Südhof TC. Distribution of synaptic vesicle proteins in the mammalian retina identifies obligatory and facultative components of ribbon synapses. Eur. J. Neurosci 1999;11:1335–1348. [PubMed: 10103129]
13. Sheng Z, et al. Synaptic Ca^{2+} in darkness is lower in rods than cones, causing slower tonic release of vesicles. J. Neurosci 2007;27:5033–5042. [PubMed: 17494689]
14. Rea R, Dharia A, Levitan ES, Sterling P, Kramer RH. Streamlined synaptic vesicle cycle in cone photoreceptor terminals. Neuron 2004;41:755–766. [PubMed: 15003175]
15. Nachman-Clewner M, St. Jules R, Townes-Anderson E. L-type calcium channels in the photoreceptor ribbon synapse: localization and role in plasticity. J. Comp. Neurol 1999;415:1–16. [PubMed: 10540354]
16. Taylor WR, Morgans C. Localization and properties of voltage-gated calcium channels in cone photoreceptors of *Tupaia belangeri*. Vis. Neurosci 1998;15:541–552. [PubMed: 9685206]
17. Barnes S, Hille B. Ionic channels of the inner segment of tiger salamander cone photoreceptors. J. Gen. Physiol 1989;94:719–743. [PubMed: 2482325]
18. Savchenko A, Barnes S, Kramer RH. Cyclic nucleotide–gated channels mediate synaptic feedback by nitric oxide. Nature 1997;390:694–698. [PubMed: 9414163]
19. Kaplan JH, Ellis-Davies GC. Photolabile chelators for the rapid photorelease of divalent cations. Proc. Natl. Acad. Sci. USA 1988;85:6571–6575. [PubMed: 3137570]
20. Van der Kloot W. Estimating the timing of quantal releases during end-plate currents at the frog neuromuscular junction. J. Physiol. (Lond.) 1988;402:595–603. [PubMed: 2466987]
21. Sun J, et al. A dual Ca^{2+}-sensor model for neurotransmitter release in a central synapse. Nature 2007;450:676–682. [PubMed: 18046404]
22. Lasansky A. Contacts between receptors and electrophysiologically identified neurones in the retina of the larval tiger salamander. J. Physiol. (Lond.) 1978;285:531–542. [PubMed: 217992]
23. Pang J-J, Gao F, Barrow A, Jacoby RA, Wu SM. How do tonic glutamatergic synapses evade receptor desensitization? J. Physiol. (Lond.) 2008;586:2889–2902. [PubMed: 18420706]
24. Yang XL, Wu SM. Effects of background illumination on the horizontal cell responses in the tiger salamander retina. J. Neurosci 1989;9:815–827. [PubMed: 2538583]
25. Rabl K, Cadetti L, Thoreson WB. Paired-pulse depression at photoreceptor synapses. J. Neurosci 2006;26:2555–2563. [PubMed: 16510733]
26. Snellman J, Kaur T, Shen Y, Nawy S. Regulation of ON bipolar cell activity. Prog. Retin. Eye Res 2008;27:450–463. [PubMed: 18524666]
27. Thoreson WB, Rabl K, Townes-Anderson E, Heidelberger R. A highly Ca^{2+}-sensitive pool of vesicles contributes to linearity at the rod photoreceptor ribbon synapse. Neuron 2004;42:595–605. [PubMed: 15157421]
28. DeVries SH. Exocytosed protons feedback to suppress the Ca^{2+} current in mammalian cone photoreceptors. Neuron 2001;32:1107–1117. [PubMed: 11754841]

29. Hirasawa H, Kaneko A. pH changes in the invaginating synaptic cleft mediate feedback from horizontal cells to cone photoreceptors by modulating Ca^{2+} channels. J. Gen. Physiol 2003;122:657–671. [PubMed: 14610018]
30. Morgans CW. Neurotransmitter release at ribbon synapses in the retina. Immunol. Cell Biol 2000;78:442–446. [PubMed: 10947871]
31. Sterling P, Matthews G. Structure and function of ribbon synapses. Trends Neurosci 2005;28:20–29. [PubMed: 15626493]
32. Gomis A, Burrone J, Lagnado L. Two actions of calcium regulate the supply of releasable vesicles at the ribbon synapse of retinal bipolar cells. J. Neurosci 1999;19:6309–6317. [PubMed: 10414960]
33. Lenzi D, von Gersdorff H. Structure suggests function: the case for synaptic ribbons as exocytotic nanomachines. Bioessays 2001;23:831–840. [PubMed: 11536295]
34. Parsons TD, Sterling P. Synaptic ribbon: conveyor belt or safety belt? Neuron 2003;37:379–382. [PubMed: 12575947]
35. LoGiudice L, Sterling P, Matthews G. Mobility and turnover of vesicles at the synaptic ribbon. J. Neurosci 2008;28:3150–3158. [PubMed: 18354018]
36. Heidelberger R. Adenosine triphosphate and the late steps in calcium-dependent exocytosis at a ribbon synapse. J. Gen. Physiol 1998;111:225–241. [PubMed: 9450941]
37. Schein S, Ahmad KM. A clockwork hypothesis: synaptic release by rod photoreceptors must be regular. Biophys. J 2005;89:3931–3949. [PubMed: 16169984]
38. Matthews G, Sterling P. Evidence that vesicles undergo compound fusion on the synaptic ribbon. J. Neurosci 2008;28:5403–5411. [PubMed: 18495874]
39. Glowatzki E, Fuchs PA. Transmitter release at the hair cell ribbon synapse. Nat. Neurosci 2002;5:147–154. [PubMed: 11802170]
40. Singer JH, Lassova L, Vardi N, Diamond JS. Coordinated multivesicular release at a mammalian ribbon synapse. Nat. Neurosci 2004;7:826–833. [PubMed: 15235608]
41. von Gersdorff H, Matthews G. Depletion and replenishment of vesicle pools at a ribbon-type synaptic terminal. J. Neurosci 1997;17:1919–1927. [PubMed: 9045721]
42. Moser T, Beutner D. Kinetics of exocytosis and endocytosis at the cochlear inner hair cell afferent synapse of the mouse. Proc. Natl. Acad. Sci. USA 2000;97:883–888. [PubMed: 10639174]
43. Holt M, Cooke A, Neef A, Lagnado L. High mobility of vesicles supports continuous exocytosis at a ribbon synapse. Curr. Biol 2004;14:173–183. [PubMed: 14761649]
44. Doan T, Mendez A, Detwiler PB, Chen J, Rieke F. Multiple phosphorylation sites confer reproducibility of the rod's single-photon responses. Science 2006;313:530–533. [PubMed: 16873665]
45. Yang XL, Wu SM. Response sensitivity and voltage gain of the rod- and cone-horizontal cell synapses in dark- and light-adapted tiger salamander retina. J. Neurophysiol 1996;76:3863–3874. [PubMed: 8985884]
46. Burkhardt DA. Light adaptation and photopigment bleaching in cone photoreceptors in situ in the retina of the turtle. J. Neurosci 1994;14:1091–1105. [PubMed: 8120614]
47. Schwartz EA. Responses of bipolar cells in the retina of the turtle. J. Physiol. (Lond.) 1974;236:211–224. [PubMed: 4818497]
48. Ruderman DL, Bialek W. Statistics of natural images: scaling in the woods. Phys. Rev. Lett 1994;73:814–817. [PubMed: 10057546]
49. Bowen RW, Pokorny J, Smith VC. Sawtooth contrast sensitivity: decrements have the edge. Vision Res 1989;29:1501–1509. [PubMed: 2635476]
50. Choi S-Y, et al. Encoding light intensity by the cone photoreceptor synapse. Neuron 2005;48:555–562. [PubMed: 16301173]

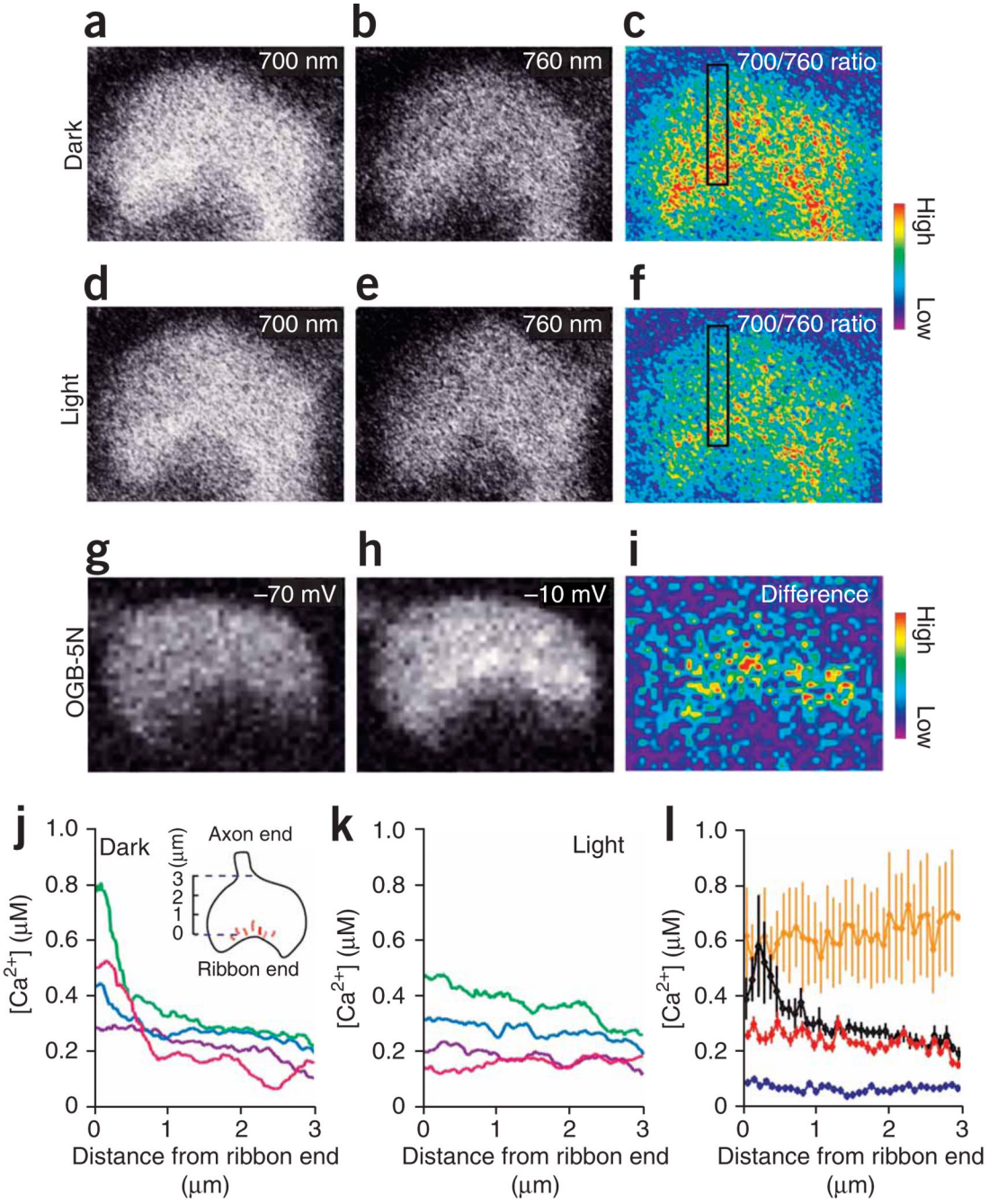

Figure 1.

Light stimulation collapses a Ca^{2+} gradient that is maintained in cone terminals in darkness. (**a**–**f**) Fluorescent images of a cone terminal in a retinal slice loaded with fura-2, collected after >10 min of dark adaptation (**a**–**c**) and a subsequent 10-min exposure to bright white light (**d**–**f**). Images from two-photon dye excitation with 700-nm light (**a**,**d**), 760-nm light (**b**,**e**) and the 700/760-nm ratio, which indicates Ca^{2+} concentration (**c**,**f**). The black box shows a 3.0 µm × 0.5 µm area for measuring the spatial profile of Ca^{2+}. The bottom area of the box is the ribbon end of the terminal and the top area is the axon end. (**g**–**i**) Images of another cone terminal showing a local increase in Ca^{2+} evoked by depolarization, measured with OGB-5N (excitation wavelength 488 nm). Intraterminal Ca^{2+} at −70 mV (**g**) after a 100-ms depolarization to −10

mV (**h**) and the difference in Ca^{2+} induced by depolarization (**i**) are shown. (**j**,**k**) Representative Ca^{2+} profiles from four terminals in darkness (**j**) and after light stimulation (**k**) measured from two-photon ratiometric fura-2 images as in **c** and **f**. Data are color coded to allow for comparison of the same terminals in darkness and light. Data points are running averages of 30 pixels binned over 500 nm. (**l**) Average Ca^{2+} profiles in cone terminals in retinal slices exposed to darkness (black), light (red), ionomycin (orange) and Ca^{2+}-free saline (blue). n = 5–12 terminals for each condition. Error bars represent s.e.m.

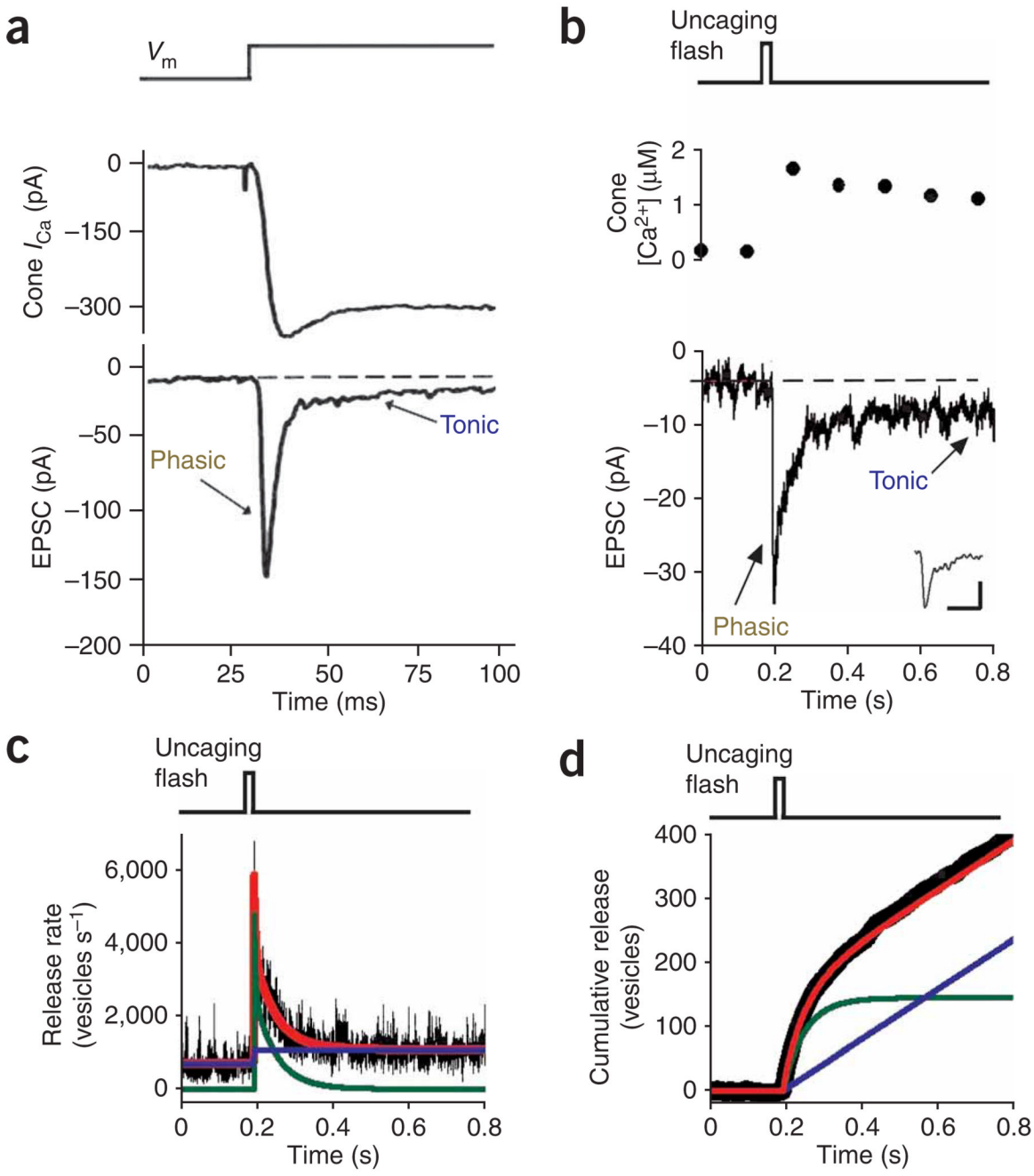

Figure 2.

Elevation of cone terminal Ca^{2+} reveals two kinetic components of release. (**a**) Simultaneous whole-cell recordings from a salamander cone photoreceptor (cone I_{Ca}) and a postsynaptic HBC (EPSC). Depolarizing cones from −70 to −10 mV elicited a sustained inward Ca^{2+} current and triggered an EPSC with phasic and tonic components. (**b**) Flash photolysis of DM-nitrophen raised Ca^{2+} levels in a different cone terminal (top), producing an EPSC in a HBC (bottom) with phasic and tonic components. Inset shows the average mEPSC for this cone-HBC pair (scale bars represent 1 pA, 10 ms). (**c**) Deconvolution of the EPSC from **b** with the waveform of the mEPSC (inset, **b**) provided an estimate of the presynaptic release rate (black trace). Release is fit by the sum of two components (red line), phasic release (the transient

release after the flash; green line) and tonic release (the average release rate occurring 0.5–1.0 s after the flash, blue line). (**d**) Integration of the release rate from **c** yielded the cumulative number of vesicles released after the uncaging flash. The pre-flash baseline release was subtracted to remove input from all but the DM-nitrophen–loaded cone.

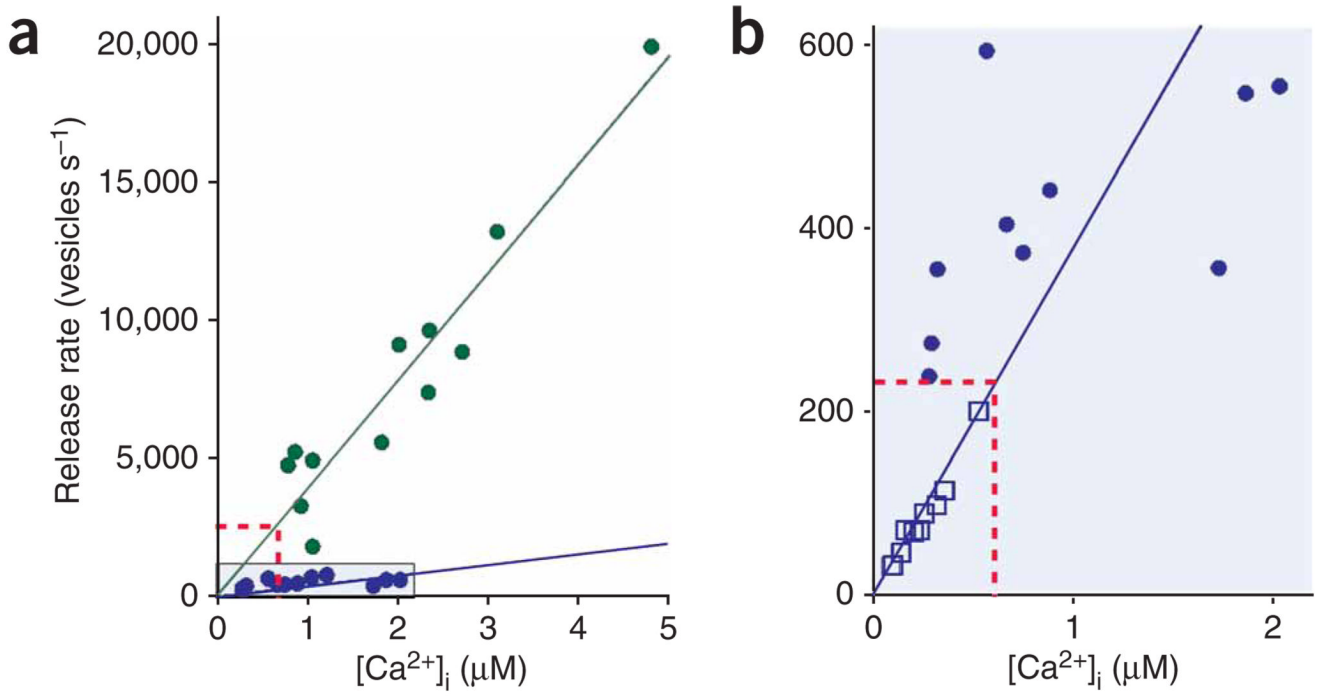

Figure 3.

Ca^{2+} dependence of phasic and tonic release. (**a**) Phasic (green circles) and tonic (purple circles) release triggered by photolytic uncaging of Ca^{2+} in cone terminals. Cone Ca^{2+} concentration was measured with OGB-6F and release was calculated by deconvolving the EPSC (see Fig. 2). (**b**) Tonic release rates determined from flash photolysis experiments (purple circles; same data points as in **a**) compared with release rates measured in anole cone terminals in which Ca^{2+} was raised slowly with ionomycin and tracked over many minutes (open purple squares). We monitored release in anole terminals with the synaptic vesicle marker FM1-43 while simultaneously measuring Ca^{2+} with fura-2. The red dotted lines show the expected rates for phasic release (**a**) and tonic release (**b**) predicted by the dark Ca^{2+} concentration (600 nM).

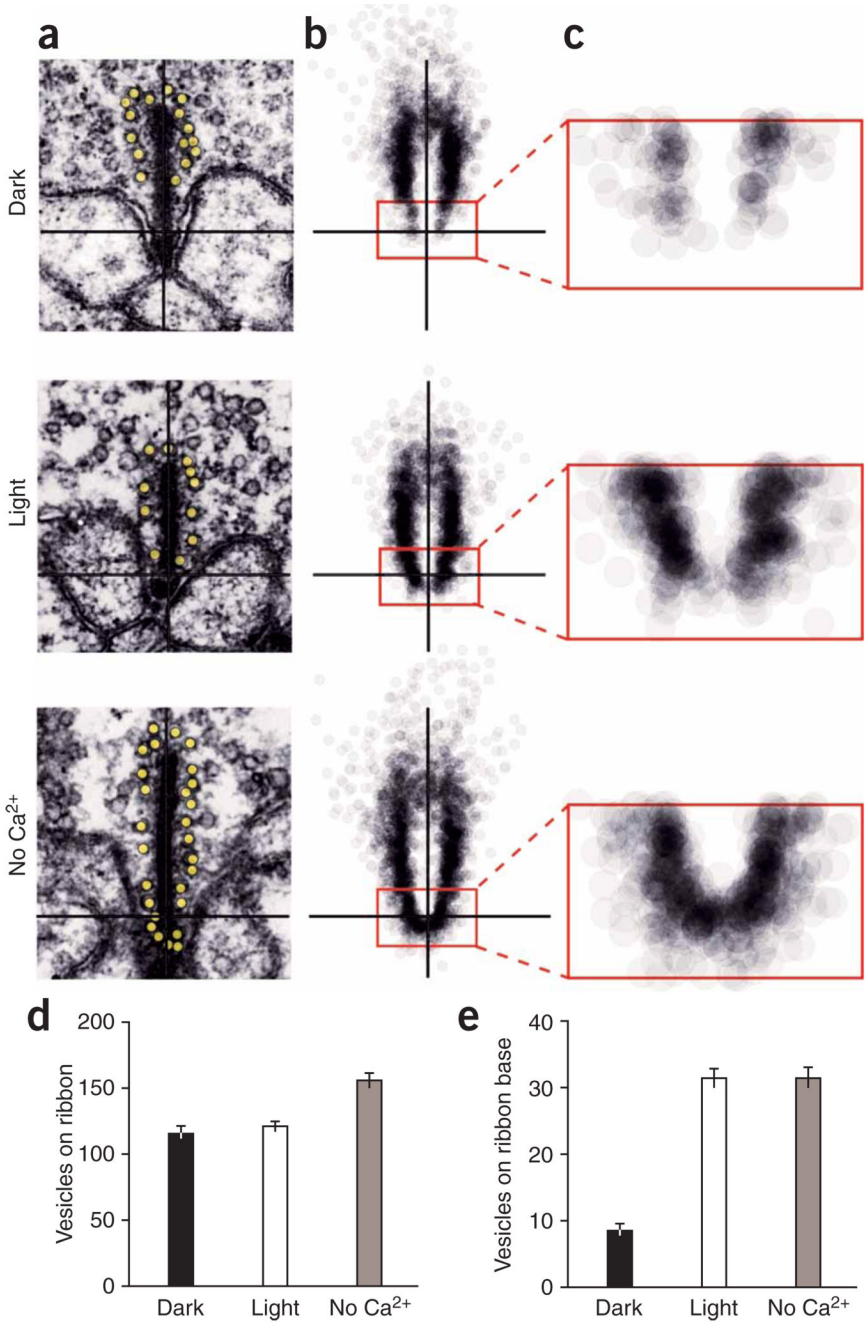

Figure 4.

Electron microscopy of ribbon-associated vesicles. (**a**) Electron microscopy pictures of cone ribbons from retina fixed in dark, light and in Ca^{2+}-free saline. (**b**) The positions of ribbon-associated vesicles from 115 ribbons were mapped and overlaid for each condition (inset rectangle = 200 nm × 400 nm). (**c**) Magnification of inset from **b**. The resultant cloud of vesicles revealed depletion near the base of the ribbon in darkness. (**d**,**e**) Vesicle occupancy of the entire ribbon (**d**) and the base of the ribbon (**e**). Average values ± s.e.m. *n* = 115 ribbons for each condition.

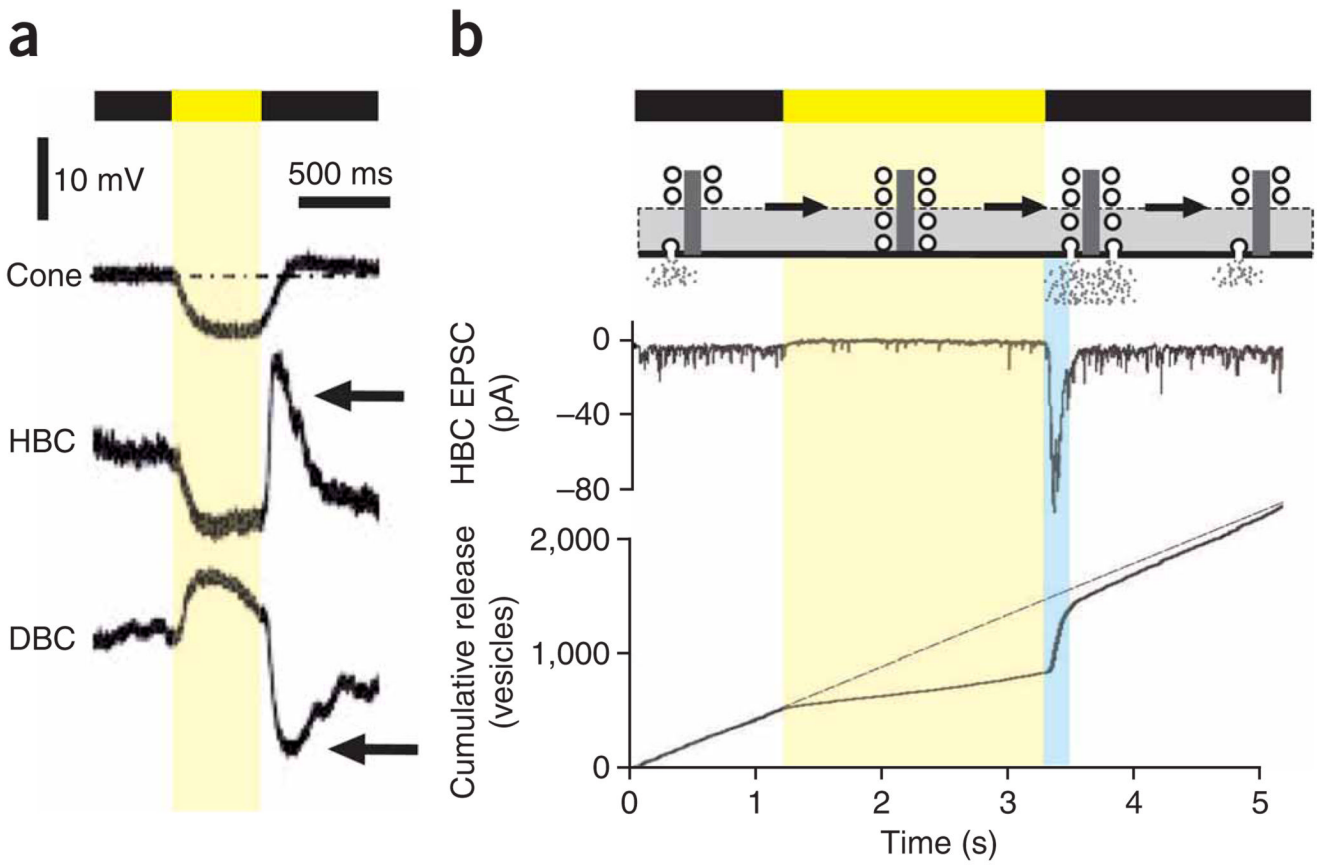

Figure 5.

Phasic release of resupplied vesicles on ribbons underlies the off response of postsynaptic neurons. (**a**) Light-evoked voltage responses from a cone, a HBC and a DBC recorded from salamander retinal slices. Postsynaptic cells, but not the cone, showed a marked overshoot of the dark membrane potential at light offset. (**b**) Predicted changes in vesicle occupancy on the ribbon before, during, and after a light flash (top). A synaptic current response to a light flash in a voltage-clamped HBC (middle) is shown. Bottom, the time course of presynaptic release from the group of cones driving this HBC. Release was calculated by deconvolving the EPSC with the waveform of the averaged mEPSC. The dotted line is fit to tonic release before the light flash.

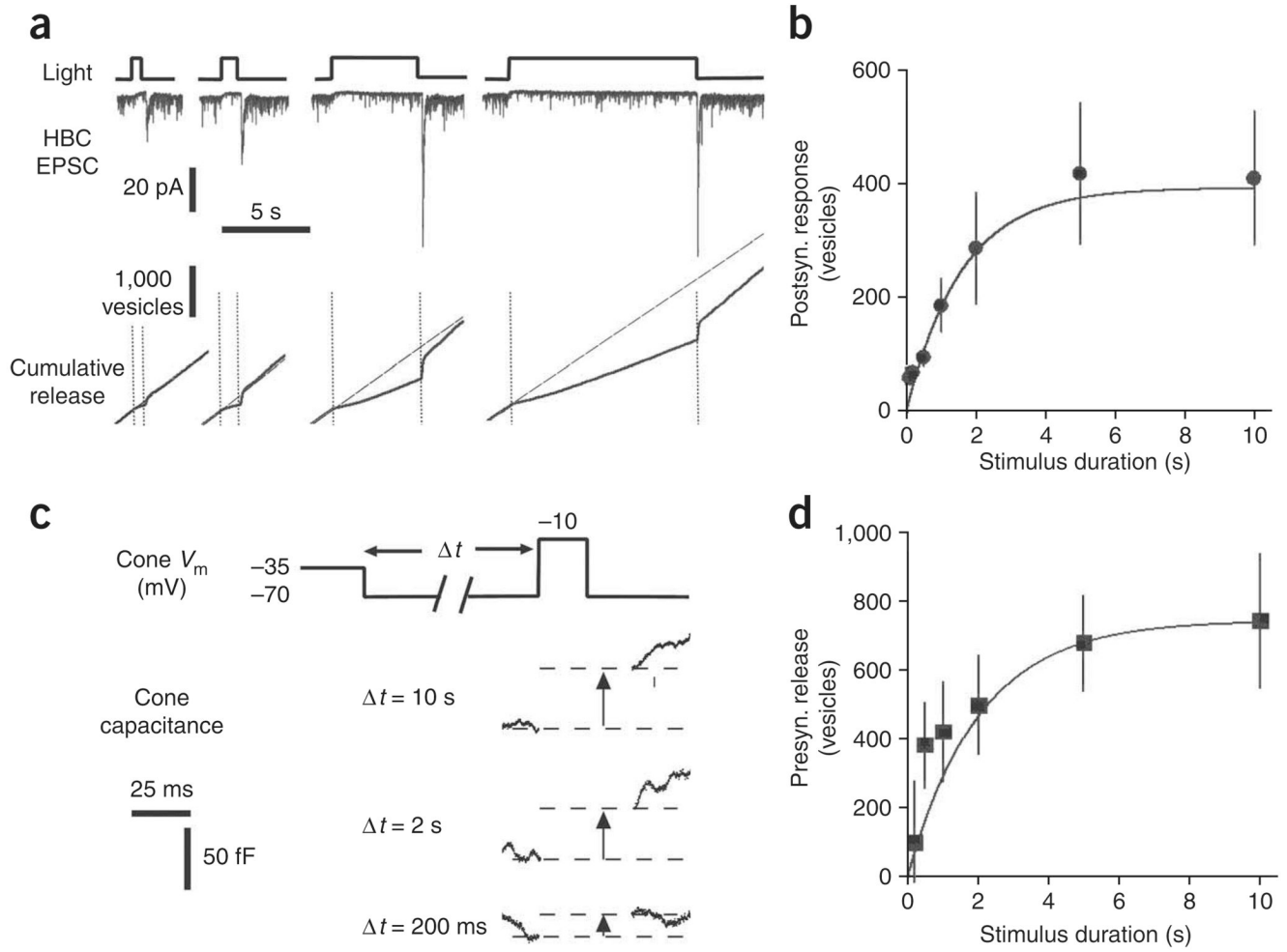

Figure 6.

The kinetics of vesicle resupply on the ribbon. (**a**) Postsynaptic responses (EPSCs) of a voltage-clamped HBC to light flashes of 0.5, 1, 5 and 10 s (top). Presynaptic release from cones was calculated by deconvolving EPSCs. Release was integrated to reveal changes in cumulative release during and after the light flashes (bottom). The diagonal dotted lines indicate the linear fits to tonic release before the light flash. (**b**) Vesicles released during the off response, following light flashes of various durations (black circles, $n = 5$), and the growth of the releasable pool predicted by the resupply model (solid line). (**c**) Quantification of exocytosis from cones using capacitance measurements. Cones were subjected to a 'simulated light flash' voltage protocol and then depolarized to elicit fusion of the releasable pool of vesicles. (**d**) Growth of the releasable pool of vesicles during the simulated light flash (squares, $n = 9–10$) and the growth of the releasable pool predicted by the resupply model (solid line). Error bars represent s.e.m.

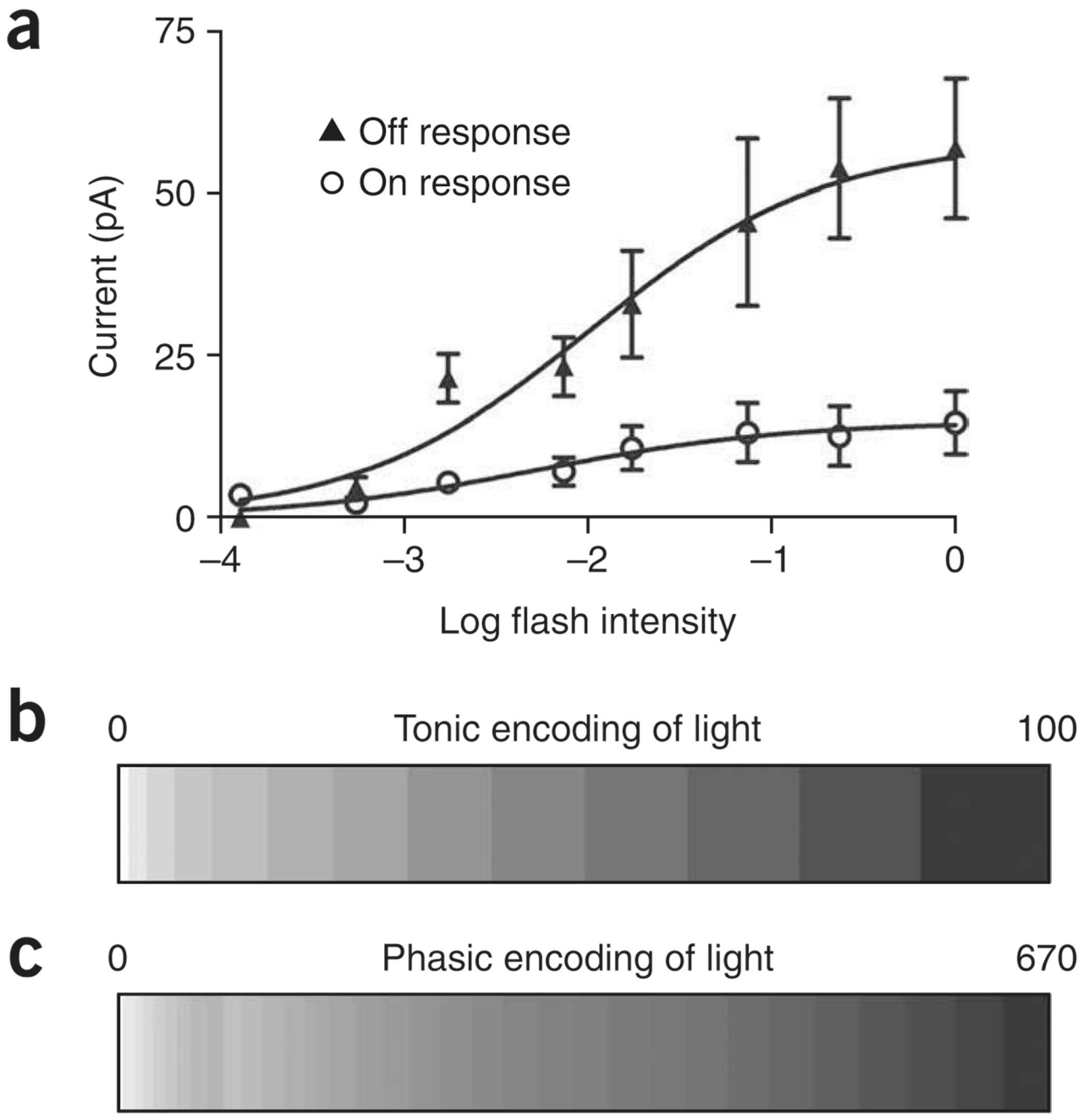

Figure 7.

Phasic release improves the encoding of a change in luminance. (**a**) Postsynaptic responses were recorded in voltage-clamped HBCs for a range of flash intensities. For both the on response (open circles) and the off response that followed a 2-s flash (solid triangles), the postsynaptic response increased over ~4 log units before saturating with very bright light. (*n* = 4–7 for each condition). (**b**) Tonic release from cone synapses could encode 13 distinguishable levels of brightness, given stochastic dark release of 500 vesicles per s (100 vesicles in the 200-ms integration time of postsynaptic bipolar cells). (**c**) Phasic release could encode 33 distinguishable levels of brightness, given a phasic release rate of ~3,350 vesicles per s (670 vesicles in the 200-ms bipolar cell integration time). Error bars represent s.e.m.